

Comparison of thermomagnetic history effects in weakly pinned single crystals of $R_3Rh_4Sn_{13}$ ($R = Yb, Ca$)

S SARKAR¹, S RAMAKRISHNAN¹, A K GROVER¹, C V TOMY²,
G BALAKRISHNAN³ and D M^cK PAUL³

¹Tata Institute of Fundamental Research, Homi Bhabha Road, Mumbai 400 005, India

²Department of Physics, Indian Institute of Technology, Powai, Mumbai 400 076, India

³Department of Physics, University of Warwick, Coventry CV4 7AL, UK

Email: shampa@tifr.res.in

Abstract. A comparative study of the thermomagnetic memory effects of J_c in two weakly pinned low T_c superconductors, $Ca_3Rh_4Sn_{13}$ (CaRhSn) and $Yb_3Rh_4Sn_{13}$ (YbRhSn), is presented. In both the systems, the peak effect (PE) phenomenon appears as an order–disorder transformation through stepwise amorphization of the flux line lattice (FLL). However, in CaRhSn, we can witness another disorder-driven transition (Bragg glass (BG) to a vortex glass (VG)) in a distinct manner as in a single crystal of high T_c $YBa_2Cu_3O_{7-\delta}$ for $H\parallel c$.

Keywords. Weakly pinned $R_3Rh_4Sn_{13}$; thermomagnetic history effects; peak effect; amorphization of flux line lattice; order–disorder transition.

PACS Nos 74.25.Dw; 74.60.Ge

1. Introduction

$Ca_3Rh_4Sn_{13}$ ($T_c \approx 8.2$ K) and $Yb_3Rh_4Sn_{13}$ ($T_c \approx 7.6$ K) are two isotropic, low T_c superconductors, belonging to the same family of ternary rare earth stannides. $Yb_3Rh_4Sn_{13}$ contains the rare earth Yb ion whereas the absence of any rare earth ions in $Ca_3Rh_4Sn_{13}$ and its very small normal state paramagnetic value of 3.3×10^{-6} emu/cm³ precludes the realization of a generalized-Fulde–Ferrel–Larkin–Ovchinnikov (GFFLO) state [1] in it. Recently, we have observed anomalous modulations (second magnetization peak (SMP) and/or the peak effect (PE)) in the macroscopic critical current density J_c in both these systems, where the characteristic internal structures span the entire PE regime. The PE has been considered as a disorder-driven order-to-disorder transition, where the collapse of the shear modulus makes the FLL softer, and more susceptible to underlying pinning. On the other hand, the origin of the SMP is mainly disorder-induced. These two anomalies (SMP and PE) are also accompanied with many accessible metastable vortex configurations carrying different current densities J_c . It is therefore instructive and interesting at this juncture

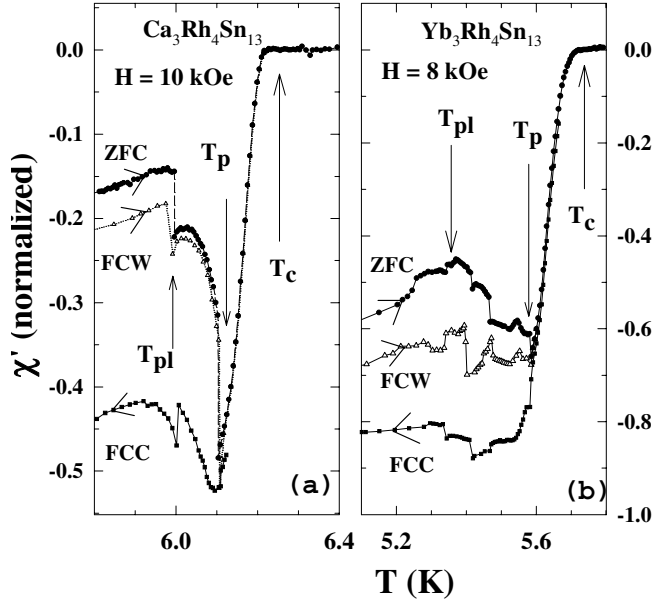


Figure 1. Isofield $\chi'_{ac}(T)$ in CaRhSn (a) and YbRhSn (b) for three sample histories (ZFC, FCW and FCC).

to perform a systematic and a comparative study of the thermomagnetic history effects of J_c in these two systems.

2. Experimental

The ac susceptibility experiments have been carried out in a home-built ac susceptometer, whereas the dc magnetization measurements have been performed using a commercial vibrating sample magnetometer (VSM). Both CaRhSn and YbRhSn have narrow fluctuation regions in the (H, T) phase space (Ginzburg number $G_i \sim 10^{-7}$) [2]. However, both these systems are weakly pinned ($j_c/j_0 \sim 10^{-5}$) and are considered suitable for examining the structural and dynamic behavior of the flux line lattice (FLL) within the frame work of the Larkin–Ovchinnikov (LO) collective pinning theory [3].

3. Results and discussion

Figures 1a and 1b display the typical isofield $\chi'(T)$ response for three thermomagnetic histories (zero field-cooled (ZFC), field cooled warm-up (FCW) and field-cooled cool-down (FCC)) in a field of 10 kOe and 8 kOe for CaRhSn and YbRhSn, respectively. The screening $\chi'(T)$ responses in both the systems show characteristic history: FLL in the FCC mode gives the largest diamagnetic screening response as compared to those in the states

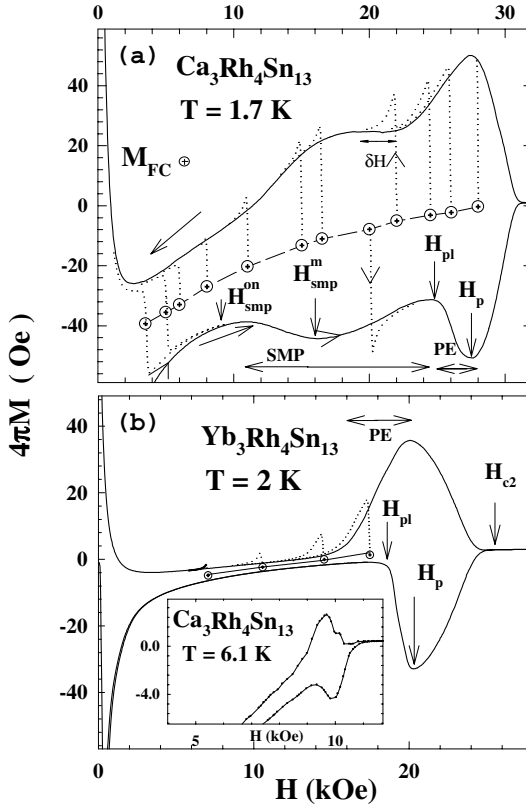


Figure 2. M - H loops for CaRhSn (a) and YbRhSn (b). Inset in panel (b) shows the M - H loop in CaRhSn at 6.1 K, where only the PE is evident.

produced via the FCW and the ZFC modes over a wide range of temperature up to the peak position of the PE. Since J_c is directly related to the $\chi'(T)$ response ($\chi' \sim -1 + ah_{ac}/J_c$), the differences in the values of $\chi'(T)$ between the ZFC, FCW and FCC modes reveal the history dependence of J_c in those modes, i.e., $J_c^{\text{FCC}}(T) \geq J_c^{\text{FCW}}(T) \geq J_c^{\text{ZFC}}(T)$ for $T \leq T_p$. While the anomalous variation in J_c in CaRhSn consists of two discontinuous transitions at T_{pl} and T_p across the PE in accordance with a stepwise amorphization/pulverization of the FLL, this process occurs in YbRhSn through multiple steps, as evident from figure 1b.

Figure 2 shows the isothermal dc magnetization hysteresis loops for CaRhSn and YbRhSn at fixed temperatures of 1.7 K and 2 K, respectively. According to the critical state model, any anomaly in J_c reveals itself as a modulation in the hysteresis width ($\Delta M(H)$) of the magnetization loop. As per the description of the LO collective pinning theory ($J_c \propto V_c^{-1/2}$, $V_c =$ correlation volume), anomalous modulations in J_c in turn reflect the transformation in V_c across respective phase boundaries. Figure 2b shows that for YbRhSn , this anomalous variation in $\Delta M(H)$ occurs near H_{c2} and can be identified as the classical PE. However, the hysteresis loop for CaRhSn in figure 2a shows an additional

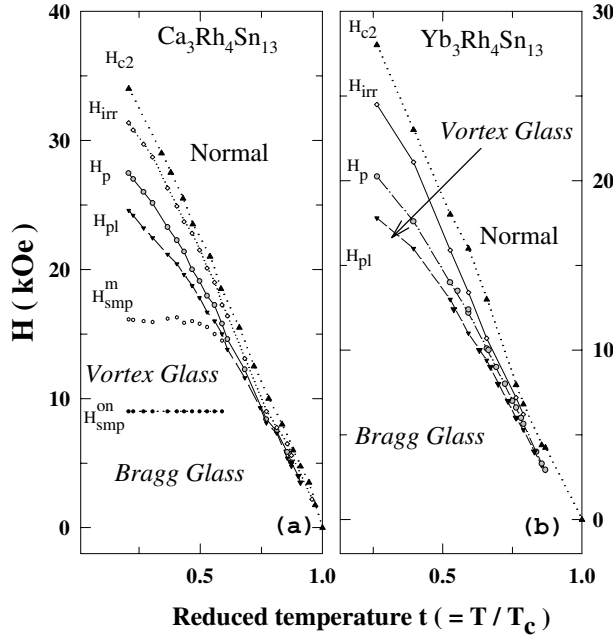


Figure 3. Vortex phase diagrams for CaRhSn (a) and YbRhSn (b), respectively.

anomaly in $\Delta M(H)$, well below H_{c2} . Following the nomenclature from the literature, this anomaly can be termed as the second magnetization peak (SMP), which has been ubiquitously reported in high T_c superconductors (HTSC). Like in HTSC, the loci of fields marking the onset and the peak fields of the SMP in CaRhSn do not show any temperature dependence. On the other hand, the loci of the fields marking the PE vary with temperature in a manner such that above 4.5 K the SMP is completely subsumed by the PE (see the inset panel in figure 2b for $M-H$ data at 6.1 K in CaRhSn). The appearance of the SMP in CaRhSn is new in the context of observations in low T_c superconductors. The dotted minor hysteresis curves in both the panels of figure 2 demonstrate the path dependences in $J_c(H)$ across the SMP and the PE regions. The minor curves in figure 2 were obtained from the vortex states prepared in the field-cooled (FC) manner. For $H < H_{SMP}^{on}$, the FC-minor curves undershoot the envelope loop (ZFC curve), but they start to overshoot as H exceeds H_{SMP}^{on} . As H approaches H_p , the FC-minor curves readily merge into the envelope loop, as the metastability and memory effects disappear above the peak position of the PE.

Collating all the data, we finally construct the vortex phase diagrams, as shown in figure 3. Note that the SMP in CaRhSn has caused the presence of the Bragg glass (BG) to the vortex glass (VG) phase boundary across which the dislocations first permeate spontaneously. The Larkin domains in the VG region could undergo a modulation (i.e., healing) between H_{SMP}^m and H_{pl} . Above H_{pl} , the Larkin domains pulverize through a two-step process. Since the SMP is not observed in YbRhSn, the phase boundary between BG to VG is absent in its phase diagram, and the fracturing of the BG proceeds through a multi-step process between H_{pl} and H_p .

Acknowledgements

One of us (SS) would like to acknowledge the TIFR Endowment Fund For the partial financial support in the form of Kanwal Rekhi Career Development Award.

References

- [1] R Modler *et al*, *Phys. Rev. Lett.* **761**, 1292 (1996)
M Tachiki *et al*, *Z. Phys.* **B100**, 369 (1996)
- [2] C V Tomy *et al*, *Phys. Rev.* **B56**, 8346 (1997)
C V Tomy *et al*, *Physica* **C280**, 1 (1997)
- [3] A I Larkin and Y N Ovchinnikov, *J. Low Temp. Phys.* **34**, 409 (1979)
- [4] S Sarkar *et al*, *Phys. Rev.* **B61**, 12394 (2000)
S Sarkar *et al*, *Physica* **C356**, 181 (2001)